Hydrodynamic and anthropogenic disturbances co-shape microbiota rhythmicity and community assembly within intertidal groundwater-surface water continuum

Ze Zhao[1, 2, 3], Lu Zhang[2, 3], Guoqing Zhang[2, 3], Han Gao[2, 3], Xiaogang Chen[2, 3], Ling Li[2, 3], Feng, Ju[2, 3, 4, 5*]

[1] College of Environmental & Resources Sciences, Zhejiang University, Hangzhou 310058, China

[2] Key Laboratory of Coastal Environment and Resources of Zhejiang Province, School of Engineering, Westlake University, Hangzhou 310030, Zhejiang Province, China

[3] Institute of Advanced Technology, Westlake Institute for Advanced Study, Hangzhou 310024, Zhejiang Province, China

[4] Center of Synthetic Biology and Integrated Bioengineering, School of Engineering, Westlake University, Hangzhou 310030 Zhejiang Province, China

[5] Westlake Laboratory of Life Sciences and Biomedicine, Hangzhou, Zhejiang Province, China

*Corresponding to:

Dr. Feng Ju (Assistant Professor)

Tel: 571-87380995

Fax: 0571-85271986

E-mail: jufeng@westlake.edu.cn

Address: E2-326, Westlake University YUNGU CAMPUS, No.600 Dunyu Road, Sandun Town, Xihu District, 310030, Hangzhou, Zhejiang Province, China

Abstract

Tidal hydrodynamics drive the groundwater-seawater exchange and shifts in microbiota structure in the coastal zone. However, how microbiota structure responds to periodic tidal fluctuations and anthropogenic disturbance is seldom evaluated in the intertidal groundwater-surface water (GW-SW) continuum, although it affects microbially driven biogeochemical cycles and ecosystem function therein. Here, we resolved the high-resolution spatiotemporal dynamics and assembly mechanisms along a GW-SW continuum in the natural tidal creek. Our results revealed an evident rhythmic pattern of microbiota structure in response to daily and monthly tidal fluctuations in intertidal surface water. The similarity in archaeal community structures among groundwater and ebb-tide surface water demonstrated archaeal transport through groundwater discharge, whereas multi-source transport mechanisms led to the occurrence of unique bacterial biota in ebb-tide water. Mechanistically, homogeneous selection (58.6%-69.3%) dominated microbiota assembly patterns in the intertidal GW-SW continuum, while biotic interactions were weaker in the groundwater microbiota than the surface water microbiota. Compared with the natural tidal creek, we found that microbiota biodiversity and community succession in intertidal groundwater under anthropogenic-induced terrestrial nutrient inputs and weakened tidal fluctuations were primarily controlled by increased dispersal limitation and consequent weakening of homogeneous selection, as well as enhanced biotic interactions. Overall, this study sheds light on the ecological rules guiding water microbiota assembly in the coastal transition zones and highlights periodic hydrodynamic and anthropogenic disturbances as prominent influencing factors of the microbiota structure, as well as the potential for enhancing coastal monitoring initiatives by incorporating only a few rhythmic but critical key microbial observations.

Key Words: Microbiota rhythmicity, Community assembly, Intertidal groundwater-surface water continuum, Tidal hydrodynamics, Anthropogenic disturbance

1. Introduction

Coastal ecosystems (e.g., salt marshes and mangroves) play a critical role in global climate regulation [1] and biogeochemical cycles [2, 3], yet they are currently facing a multitude of local and global challenges caused by climate change and human activities (e.g., pollution). In addition to the well-known river-runoff input and atmosphere deposition, submarine groundwater discharge (SGD) or porewater exchange in coastal aquifers has been proven to be an essential source of nutrients and other pollutants to the ocean [4, 5]. Meanwhile, the coastal aquifers harbor a large diversity of microorganisms that are transported and dispersed via SGD and key drivers of biogeochemical cycles within the groundwater-seawater mixing system [6]. Most existing studies have focused on microbiota structure in only one compartment of intertidal zone, such as coastal sediment [7], groundwater or coastal seawater [8-11]. However, microbiota structure and dynamics in the intertidal groundwater-surface water (GW-SW) continuum, especially in the context of the high structural variability and complexity associated with SGD and microbial transport, remain poorly explored. Moreover, while periodic disturbances (e.g., tidal fluctuation) are revealed to influence the microbiota structure in various environments [12, 13], high-resolution profiling of microbiota dynamics is missing but required to resolve their roles in the community structuring sensitively. Therefore, the high-resolution time series profiling, e.g., on a daily or monthly basis of tidal cycles, would help resolve the microbiota dynamic patterns and assembly rules in the intertidal aquatic continuum and further identify whether or which processes and factors may govern the microbiota structuring and

ecosystem function.

Hydrodynamic disturbance can cause steep variations in physicochemical conditions over short spatial or temporal scales, thus it is often regarded as a critical factor controlling microbiota assembly and biogeochemical processes in coastal sediments [12]. Various environmental factors (e.g., salinity, pH, temperature and nutrient [8, 14-17]) are implicated in exerting selective pressures on the intertidal groundwater or coastal seawater microbiome. The results are broadly consistent with the niche-based theory, which asserts that deterministic processes such as environmental filtering and biotic interactions largely control the patterns of microbiota composition and distribution [18]. Furthermore, according to the well-established community assembly theory [19, 20], microbiota structure and succession are controlled by four fundamental ecological processes: selection, dispersal, drift and speciation (or diversification), which vary in their degree of determinism and stochasticity [21]. Based on quantitative analysis through the null model [22, 23], until now, only a few studies have reported on the microbiota assembly patterns in the intertidal sediment [17, 24, 25] or coastal seawater [26], but the relative contribution of each ecological process (i.e., homogeneous selection, dispersal limitation and drift) greatly varied across studies. Comparatively, the microbiota assembly processes shaping community structure and succession patterns have never been quantified in the intertidal GW-SW continuum, especially that our knowledge of the role of hydrodynamic and anthropogenic disturbances is limited.

Deterministic processes, including environmental or habitat filtering and biotic interactions, are treated as joint selection forces in the community assembly and interact dynamically to drive the observed community patterns [27, 28]. However, their respective contribution cannot be parsed out based on the quantitative approach of the

null model [23]. Instead, deterministic processes and ecological relationships can be interactively and topologically explored in a microbial co-occurrence or molecular ecological network, which is fundamental for predicting microbial species interactions and niche patterns in both natural [29, 30] and engineered [31-33] ecosystems. Previous studies have reported that enhanced seawater intrusion weakened the complexity of microbial co-occurrence associations in intertidal sediment [24], whereas it strengthened microbial interactions and led to more compact microbial networks in groundwater [10]. However, microbial co-occurrence patterns in the intertidal GW-SW continuum and their dynamics under regular hydrodynamic disturbance (e.g., periodic tidal fluctuations) and increasing anthropogenic impacts (e.g., land-sourced pollutants) are almost blank. Therefore, complementing the state-of-the-art null modelling of ecological processes with community-wide co-occurrence patterns in the quantitative analyses of microbiota assembly will enable more complete insights into the major drivers underlying microbiota structuring and ecological rules guiding the community assembly and function in coastal ecosystems.

To explore the high-resolution hourly dynamics of microbiota structure and community assembly mechanisms in the intertidal aquatic continuum, we collected intertidal groundwater and time-series surface water in a natural saltmarsh tidal creek (TC2) located in Jiangsu Province, China (Fig. 1A), where mudflats were estimated to cover more than 90% of the 954-km Jiangsu coast [34]. Meanwhile, a geographically adjacent but human-influenced tidal creek (TC1) was chosen and compared with TC2 to resolve the anthropogenic influence on intertidal groundwater microbiota. The objectives of this study are: (i) to investigate the temporal dynamics of microbiota structure in intertidal surface water with daily and monthly tidal fluctuations; (ii) to explore the processes and mechanisms in microbiota assembly in intertidal GW-SW

continuum under hydrodynamic disturbance; and (iii) to elucidate anthropogenic influence on the spatial distribution and community assembly of intertidal groundwater microbiota. This study will provide the first and in-depth understanding of microbiota dynamics and assembly mechanisms of the intertidal water continuum co-shaped by hydrodynamic and anthropogenic disturbances in the coastal ecosystem.

2. Materials and Methods

2.1. Field sample collection and physicochemical analysis

Samples were collected from the Saltmarsh Tidal Creeks (Fig. 1A and Fig. S1) located at Dafeng Milu National Nature Reserve, Yancheng City, Jiangsu Province, China, between August 4th and August 15th, 2020 (Table S1). Groundwater was collected from the intertidal zone of tidal creek 1 (8 samples for TC1) and tidal creek 2 (12 samples for TC2) at a depth of 1.0-1.5 m. The outlet of TC1 is connected to the estuary of the Chuandong River and the estuarine water flows into TC1 at flood tide. Besides, the terrestrial river upstream of TC1 discharges water into the creek at ebb tide, which is controlled by a floodgate. On the contrary, the downstream mouth of TC2 is about 4.5 km away from the Chuandong estuary with no water input from terrestrial river or aquaculture, indicating rare anthropogenic influence and is therefore considered a natural tidal creek.

In addition, time series sampling of tidal creek surface water was performed to investigate the impact of periodic tidal fluctuations. Water samples were collected hourly from the Time Series Station (TS) downstream of TC2 (Fig. S2), covering two whole tidal cycles during the neap (N1-N14 on August 12th) and spring tide (S1-S15 on August 6th-7th). Each water sample (300-1400 ml) was filtered on-site through 0.2 μm pore size polycarbonate filters (Millipore, USA) for about 30 minutes. The filters were

transported to the laboratory with dry ice in 24 h and stored at -20 °C until DNA extraction. Physiochemical properties, including water depth, temperature (temp), pH, salinity, dissolved oxygen (DO), dissolved organic and inorganic carbon (DOC and DIC), and ^{222}Rn (groundwater isotope tracer) of water samples were measured according to our earlier publication [35] (detailed in Supplementary Text S1).

In total, 49 water samples were grouped for further analysis based on their sources and sampling times as follows: (i) intertidal groundwater collected from TC1 (TC1-PW) and TC2 (TC2-PW); (ii) time-series surface water samples grouped according to two different grouping rules, namely TS-Neap and TS-Spring samples collected during neap tide and spring tide, or TS-Ebb and TS-Flood samples collected during ebb tide and flood tide designated by the *in-situ* observation of water depth.

2.2. DNA extraction, qPCR and 16S rRNA gene sequencing

Total genomic DNA was extracted using DNeasy PowerSoil Kit (Qiagen, Germany). The V4-V5 regions of prokaryotic 16S rRNA genes were amplified using primers 515F and 926R, and sequenced on the Illumina NovaSeq 6000 platform with 250-bp paired-end reads at the Magigene Biotechnology Co. Ltd (Guangzhou, China). The raw sequencing data were processed following the Qiime2 pipeline [36] described in Supplementary Text S2. Then the table of amplicon sequence variants (ASVs), taxonomy and tree files were processed by R library phyloseq [37], MicrobiotaProcess and microeco [38]. Briefly, ACE and Shannon indices were used to evaluate the alpha-diversity of microbial communities. To analyze beta-diversity, all sequences were standardized to the median sequencing depth using the phyloseq function *transform_sample_counts.* The non-metric multidimensional scaling (NMDS) analysis and permutational multivariate analysis of variance (PERMANOVA) was performed based on weighted UniFrac distance. The Lomb Scargle periodogram (LSP) was used

to determine if rhythmic patterns were present in microbial ASVs [39], as described in Supplementary Text S3.

2.3. Community assembly processes of tidal creek water microbiota

A recently proposed framework 'iCAMP' was used to quantify the contribution of different ecological processes to community assembly based on phylogenetic bin-based null model analysis [22, 23]. The observed taxa were first divided into different 'bins' and the relative importance of heterogeneous selection, homogeneous selection, homogenizing dispersal, dispersal limitation, and drift in individual 'bins' was calculated to evaluate the dominated 'bins' and dominated taxa contributing to the ecological processes. In brief, 37294 observed ASVs were divided into 687 phylogenetic bins (renamed as Bin1, Bin2, *etc.*). Phylogenetic tree of 300 most abundant Bins (89.6-97.9% of total contribution to community assembly) and the relative importance of ecological processes in each Bin were displayed by an online tool 'iTOL' [40]. Furthermore, all 687 Bins were grouped based on their top member lineage at class level, named 'Bin-class'. Contributions of the Top 15 and other Bin-class to dominant ecological processes among groups were visualized by R package 'pheatmap' [41]. In addition, Mantel tests with constrained permutations were performed to reveal the correlations between individual processes and various environmental factors and the scripts are publicly available from GitHub of 'iCAMP' [22]. Both linear and general linear models were tested and each factor was either log-transformed or not to explore the best model.

2.4. Checkerboard score and co-occurrence network analysis

The checkerboard score (C-score) model was used as the metric of species segregation and its variance (C_{var}-score) was used as the metric of both species segregation and

aggregation in the intertidal water microbiota [42, 43]. The higher the observed standardized effect (SES) values of C-score, the greater degree of species segregation relative to a random distribution. The C-score tests were performed using the scripts of package MbioAssy1.0 (https://github.com/emblab-westlake/MbioAssy1.0) [31] and more information can be found in Text S4. The co-occurrence network and global network properties were generated using the Molecular Ecological Network Analysis Pipeline [44, 45] and visualized with Gephi v0.9.2. Six networks were constructed based on abundance profiles of ASVs that present in at least half of the samples of each sample group. The resulting correlation matrix (Pearson correlation coefficient) was analyzed with the random matrix theory- (RMT-) based approach to determine the correlation threshold. Moreover, the 1000 corresponding Erdös-Réyni random networks, the small-world coefficient (σ) and the keystone nodes were generated for each network and more details are described in Supplementary Text S5.

3. Results

3.1. Microbiota diversity and structural variations in intertidal water continuum

We first investigated the diversity and structural variations of prokaryotic (i.e., archaeal and bacterial) communities in intertidal groundwater and surface water. Based on ACE and Shannon indices (Wilcoxon rank-sum test, $p < 0.05$, Fig. 1B), archaeal alpha-diversity in the natural tidal creek groundwater (TC2-PW) was significantly higher than (TS-Flood and TS-Spring) or equal to (TS-Ebb and TS-Neap) that in the surface water, whereas bacterial alpha-diversity showed a reversed trend, i.e., lower in the TC2-PW group than the TS-Ebb, TS-Neap and TS-Spring groups, and equal to the TS-Flood group. Comparatively, human-influenced creek groundwater (TC1-PW) harbored significantly higher prokaryotic alpha-diversity than not only the groundwater (TC2-

PW) but also the surface water (TS) of the natural creek.

When weighing relative abundance, archaeal communities were significantly more abundant in the human-influenced creek groundwater (TC1-PW: 1.76%-49.66%) than the natural one (TC2-PW: 0.56%-14.25%) (Wilcoxon rank-sum test, $p = 0.02$, Table S2), while they were more enriched in the downstream than upstream groundwater of both creeks (Fig. S3). Overall, archaeal communities in both groundwater and surface water were mainly comprised of phylum Nanoarchaeota (12.0-76.4%), Crenarchaeota (6.2-67.0%), Thermoplasmatota (0.3-9.3%), and Halobacterota (0.3-53.0%), which showed remarkably dynamics of relative abundance in broad ranges and across sampling groups (Fig. 1C). For example, family Woesearchaeales and SCGC AAA011-D5 were the most abundant Archaea in TC-PW and TS-Ebb groups, whereas family Nitrosopumilaceae and Marine Group II (typical seawater archaea) were most abundant in TS-Flood group (Fig. S4). Notably, up to 9.8% of unclassified archaea were detected in groundwater, suggesting the prevalence of numerous yet-to-be-characterized 'archaeal dark matter' in the coastal zone. Moreover, we observed weak but significant structural differences (PERMANOVA, $R^2 = 0.14$, $p = 0.02$, Table S3) in archaeal communities between TC1-PW and TC2-PW groups (Fig. 2A), as well as higher community dissimilarities within TC1-PW group (Wilcoxon rank-sum test, $p < 0.05$). The dynamics of archaeal community structure in the surface water were strongly related to tidal cycles, with similar archaeal structure observed among TC2-PW and TS-Ebb groups ($R^2 = 0.06$, $p = 0.202$) and significant variations between TS-Ebb and TS-Flood groups ($R^2 = 0.60$, $p < 0.001$), which was further confirmed by NMDS ordinations in Fig. 2A. This expected result well reflected the microbial transport through SGD: i) the transport of groundwater microbes to surface water via groundwater discharge at ebb tide and ii) the transport of coastal microbes to intertidal

surface water via seawater intrusion at flood tide.

Echoing archaeal communities, bacterial communities in the groundwater showed significant structural differences between human-influenced (TC1-PW) and natural (TC2-PW) tidal creeks (R^2 = 0.16, p = 0.002), as well as lower community dissimilarities within the natural creek (TC2, Fig. 2B). The overall groundwater bacterial communities were dominated by Proteobacteria (19.0-82.7%), Bacteroidota (1.8-40.7%) and Campilobacterota (1.5-39.7%), while the surface water communities were dominated by Proteobacteria (28.8-71.5%), Bacteroidota (5.5-21.4%), Cyanobacteria (1.2-39.7%), Actinobacteriota (6.8-22.5%) and Planctomycetota (0.8-22.5%) (Fig. 1D). Unlike archaea, bacterial communities were structurally different among TC2-PW, TS-Ebb, and TS-Flood groups (R^2 = 0.46-0.58, $p < 0.01$, Table S3), as illustrated by their clearly separate clusters in the NMDS diagram (Fig. 2B). Besides, PERMANOVA analysis also showed significant community structural differences between TS-Neap and TS-Spring groups (R^2 = 0.15, $p < 0.01$).

3.2. Microbiota rhythm patterns in intertidal surface water

To further resolve the high-resolution temporal dynamics of surface water microbiota, we performed NMDS analysis within the surface water samples (n = 29) to investigate the time-series community structural dynamics at hourly intervals during two whole tidal cycles including neap tide (August 12th) and spring tide (August 6th-7th). Complying with our hypothesis that periodic hydrodynamic disturbance should generate microbiota rhythm patterns, we observed four clusters of surface water samples separated by ebb-flood tide and neap-spring tide with a circular trajectory (Fig. 3A), indicating rhythm patterns of microbiota structure remarkably in the surface water following daily (ebb-flood) and monthly (neap-spring) tidal cycles. The intriguing circadian rhythm patterns of microbiota dynamics were superimposed by highly

synchronized and complex bacterial community dynamics and contrastingly weak (but abrupt) and simpler archaeal community dynamics (Fig. S5).

Further, we correlated surface water microbiota structure (TS-Neap, TS-Spring, and TS groups) to eight environmental factors, i.e., water depth, temperature, salinity, pH, DO, DIC, DOC, and ^{222}Rn, to verify the afore-mentioned microbiota rhythm patterns and to identify their major environmental drivers (Fig. 3B). These environmental factors are generally regarded as indicators of tidal cycles [2], and seven of them (except for DOC) were identified to display significant rhythm patterns with tidal cycles (PNmax = 0.34-0.77 and P-value < 0.01, Table S4). Overall, the results showed that seven environmental factors, except for temperature, exhibited significant correlations with surface water microbiota collected at neap tide, spring tide or both, supporting the rhythm patterns of microbiota structure in tidal creek surface water.

Based on rhythmic testing (Lomb Scargle Periodogram (LSP) tests) of 1120 ASVs, we identified 495 rhythmic ASVs (Table S5) that spanned rhythmic periods of 10.69 to 49.86 hours, accounting for 62.5% to 88.8% of total relative abundance (Fig. S6). Moreover, the rhythmic prokaryotic subcommunities (i.e., all rhythmic ASVs) exhibited a rhythmic turnover pattern of microbiota structure (Fig. 3C) that was highly consistent with the whole communities, whereas the rhythmic pattern was not observed in the non-rhythmic subcommunities (i.e., all non-rhythmic ASVs, Fig. 3D). Within 495 rhythmic ASVs, we separated 42 ASVs with rhythmic periods of 10-14 hours (as marked in Table S5), which is approximately equal to the tidal cycle period of about 12 hours for a regular semidiurnal tide reported here. Twenty-two rhythmic ASVs were classified as potential indicators of intertidal groundwater discharge according to the detection of their higher recurrent signals at ebb tide. In turn, the other 20 ASVs with higher recurrent signals at flood tide were classified as indicators of seawater intrusion

(Fig. 3E and Fig. S7). To validate that these 42 rhythmic ASVs were useful indicators of water physiochemistry, eight random forest regression models were constructed to predict each physicochemical variable (Text S6). Linear regression models comparing the predicted to actual variables showed stronger correlations (adjusted R^2 = 0.90-0.99, Fig. S8) and regression slopes closer to 1 (0.70-0.88, which represents a perfect prediction), indicating high predictive accuracy and great differentiation between ebb-tide and flood-tide surface water samples.

3.3. Microbiota assembly processes and mechanisms in intertidal groundwater and surface water

To explore mechanisms underpinning the spatiotemporal dynamics and patterns in the intertidal GW-SW continuum, the relative contribution of five ecological processes (see methods) to the microbiota assembly was quantitatively evaluated. Overall, homogeneous selection (38.5%-69.3%), dispersal limitation (5.2%-49.0%) and drift (8.8%-22.5%) were the dominant processes that together explained 96.3% to 98.5% of community assemblage (Fig. 4A and Table S6), and therefore the subsequent analysis was focused on them. The results showed that homogeneous selection (58.6%-69.3%) predominated in the microbiota assembly of the natural GW-SW continuum, including groundwater (TC2-PW) and surface water (TS-SW). And the contribution of dispersal limitation markedly decreased in TS-Flood (5.2%) and TS-Spring (7.1%) groups. In addition, the importance of dispersal limitation dramatically increased and predominated in the human-influenced groundwater (49.0% in TC1-PW), accompanying decreased homogeneous selection (38.5%) and drift (8.8%).

Further, the above-mentioned relative importance of each ecological process was quantified down to the refined level of individual phylogenetic lineages (Bins) defined in iCAMP (Table S7) [22]. Our results revealed that homogeneous selection was

dominated in 11.4% to 13.0% of 687 Bins (Table S8), which accounted for a summed relative abundance of 49.3% to 54.1%, while dispersal limitation dominated in 26.1% to 71.0% Bins (relative abundance: 2.9%-39.2%) and drift dominated in 16.6% to 59.0% Bins (relative abundance: 10.5%-43.5%), revealing the prevalence and dominance of homogeneous selection in a few species with disproportionally higher abundance in the intertidal GW-SW continuum. By exhibiting the contribution of each Bin, we found that the contribution of a few high-abundance Bins (e.g., the sixteen Bins marked in Fig. 4B) was remarkably higher than that of others and thus cumulatively accounted for the major contribution in the microbiota assembly. For example, the most abundant Bin1 (7.3% in total abundance of Bins) contributed up to 11.6% of homogeneous selection in TC2-PW group. The results of grouping Bins at class level, i.e., 104 Bin-class (Table S9), also showed the major contribution of abundant Bin-class in the natural tidal creek (Fig. 4C). Comparatively, the enhanced dispersal limitation in the human-influenced groundwater (TC1-PW) was attributed to the jointly increased contribution of both high and low abundance Bins, which was confirmed by the higher contribution of Bin-class Nanoarchaeia (8.5%), Dehalococcoidia (3.6%), and Clostridia (1.4%) in TC1-PW for dispersal limitation (Fig. 4C). Overall, these results indicated that high-abundance microbial lineages contributed most to homogeneous selection in the natural intertidal GW-SW continuum, whereas the accumulated contributions of both abundant and rare lineages resulted in the enhanced dispersal limitation in the human-influenced groundwater.

3.4. Environmental factors influencing the ecological processes of microbiota assembly

Environmental variables associated with hydrodynamic disturbance may impose selection on microbial communities. However, they may also reflect influence of water

mixing (e.g., salinity associated with tidal cycles), which imposes dispersal on microbiota. Therefore, correlations between changes in environmental factors and dominant ecological processes among paired samples were further determined with Mantel test ($p < 0.05$) to identify the major drivers of dominant ecological processes. Overall, homogeneous selection and dispersal limitation showed statistically similar correlation patterns (Mantel test for p-value correlation matrix: r = 0.70, $p < 0.05$) with various environmental factors, while weaker and less frequent correlations were detected between drift and environmental factors (Fig. 5 and Table S10). Both homogeneous selection and dispersal limitation showed significant correlations with salinity, pH, DO, DIC and DOC in neap-tide (TS-Neap) and spring-tide surface water (TS-Spring), although weaker correlations were observed in dispersal limitation. Considering the fluctuating environmental factors with tidal flows and their significant inter-correlations (Fig. S9), the significant correlations between these factors and dispersal limitation may indicate the influence of GW-SW mixing on the temporal microbiota turnover in intertidal surface water. Moreover, the environmental factors showed similar, although weaker (except for TC1-PW, R^2: 0.05-0.42) effects on drift compared with homogeneous selection (R^2: 0.04-0.81), indicating potential co-effect of weak selection, weak dispersal, diversification and drift represented by 'drift' here [22].

Notably, the environmental factors associated with homogeneous selection were quite different in the human-influenced (DIC and DOC) and the natural (salinity, pH and DO) groundwater, and so was dispersal limitation and drift, suggesting a potential effect of carbon nutrients on the microbiota assembly in the human-influenced groundwater. Furthermore, ecological processes in TS-Flood group showed no correlations with all environmental factors except for the weak correlation between salinity and dispersal limitation, revealing potential key roles of unmeasured factors

shaping the assembly patterns in the seawater-dominated surface water.

3.5. Deterministic microbial segregation and co-occurrence patterns of tidal creek water microbiota

Once stochastic and deterministic processes are demonstrated to co-drive the microbiota assembly in the intertidal GW-SW continuum, we applied C-score and co-occurrence network analyses to explore the contribution of biotic interactions (e.g., competition and mutualism) [22] on the observed assembly patterns, which are included in selection process but could not parse out by the afore-mentioned null model analysis. Based on positive values of standardized effect size (SES) of C-score and their ranks (Fig. 6A), the observed intertidal water microbiota exhibited significant and stronger segregated distributions during Neap than Spring tide (51.2 vs 21.8), during Ebb than Flood (21.8 vs 13.2), and in TC1 than TC2 (13.9 vs 5.3), compared with those expected under 'random' null hypothesis (Table S11). Moreover, the SES values of both C-score (5.3) and C_{var}-score (3.9) were the lowest in the natural creek groundwater microbiota (TC2-PW), while their values were much higher in the human-influenced groundwater microbiota (TC1-PW; 13.9 and 11.7), revealing an overall lower degree of both species segregation and aggregation (e.g., resulted from competition and cooperation) in the natural than the human-influenced groundwater.

Because C-score analysis revealed significant roles of both cooperative (e.g., synergistic) and competitive (e.g., antagonistic) biotic interactions in microbiota assembly [46], we further explored microbial co-occurrence patterns by establishing six networks for intertidal groundwater or surface water microbiota (Fig. 6B). Topological analysis showed that the observed networks displayed significantly different topological structures from their corresponding random networks (n=100) of identical size. They all had highly modular structures (modularity > 0.4) and showed

'small-world' properties ($\sigma > 1$) with coefficients between 1.93 to 6.19 (Table S12), revealing non-random network structures and assembly patterns that were unlikely to appear due to chance. In the natural intertidal GW-SW continuum, intriguingly, a higher percentage of rhythmic ASVs was observed in each surface water network (61.5%-73.7%) than in the groundwater network (44.8%, Table S12). Meanwhile, by investigating keystone taxa (ASVs) in each network based on their topological roles (detailed in Text S5), we found that seven of the eight keystone taxa (5 module hubs and 3 connectors) identified in the surface water network were also rhythmic ASVs (Table S13). The key role of rhythmic ASVs and the afore-mentioned differences in SES values of C-score and C_{var}-score among surface water groups, suggested that tide-driven dynamics of rhythmic subcommunities mainly dominated stronger species aggregation and segregation patterns in intertidal surface water.

The anthropogenic influence on co-occurrence patterns of groundwater microbiota was comparatively explored between the human-influenced tidal creek (TC1-PW) and the natural one (TC2-PW, Fig. 6B). The number of nodes (358), number of edges (2413), graph density (0.038), and average clustering coefficient (0.491) of TC1-PW network were all remarkably higher than that of TC2-PW network (288, 713, 0.018 and 0.308, respectively), suggesting higher frequencies of species co-occurrence associations in the human-influenced than natural groundwater. Moreover, mantel tests showed that both temperature and DIC/DOC correlated positively (though not always significant) with almost all modules in TC1-PW network ($P < 0.05$, Fig. S10), whereas none of these parameters correlated with modules in TC2-PW network, suggesting they played a potential essential role in shaping the modularized structures in TC1-PW network representing discrete ecological niches in the human-influenced tide creek. Ten keystone ASVs were observed in the TC1-PW network and were all identified as

‘connector’, but only two keystone ASVs (one ‘module hub’ and one ‘connector’) were identified in the TC2-PW network (Table S13 and Fig. S11).

4. Discussion

Tidal hydrodynamics drive the groundwater-seawater exchange and shifts in microbiota structure in the intertidal zone. However, the periodic tidal fluctuations and complex geological environment make it difficult to accurately resolve the temporal dynamics of microbiota structure based on a few discrete time-series samples in this intertidal groundwater-surface water continuum. Through high-resolution time-series microbiota profiling and modeling, this study provides first insights into the microbiota rhythmic patterns in response to periodic tidal fluctuations in intertidal surface water of Yancheng, Jiangsu Province, China, and identifies homogeneous selection as the key process driving microbiota assembly in the intertidal GW-SW continuum. Furthermore, by comparing groundwater microbiota between the natural tidal creek and a nearby human-influenced one, we found that prokaryotic biodiversity and community succession in intertidal groundwater under anthropogenic influence, including terrestrial nutrient inputs and weakened tidal fluctuations, was primarily controlled by enhanced dispersal limitation and weakened homogeneous selection, as well as both increased strengths in biotic interactions in the community assembly.

4.1. Tide cycles drive periodic transport and rhythm patterns of microbiota along the natural intertidal water continuum

The high-resolution temporal dynamics of microbiota structure in tidal creek surface water were followed during whole tidal cycles. Our results showed that archaeal and bacterial communities exhibited structure differences, whether between intertidal surface water during the ebb and flood tide or neap and spring tide, revealing tidal

fluctuations shaping the daily (i.e., ebb-flood) and monthly (i.e., neap-spring) dynamics of microbiota structure. In addition, the observed similarity in archaeal community structure among intertidal groundwater and ebb-tide surface water provides evidence for the transport of archaea from intertidal groundwater to surface water via groundwater discharge. Unlike Archaea, the potentially multi-source transport mechanisms other than groundwater discharge may be responsible for the unique bacterial community structure of ebb-tide surface water that differs from the intertidal groundwater. For example, bacterial biota might also originate from the release of particle-attached bacteria via particle resuspension from surface sediments and flushing of the surficial sediment bacteria [47]. The likelihood of such events in our study is confirmed by the unique higher abundance of family Cyanobiaceae (Fig. S4) and genera *Candidatus Aquiluna*, *Roseibacillus*, *NS11-12 marine group* (Fig. S12) in the ebb-tide surface water compared to the intertidal groundwater and flood-tide surface water. The family Cyanobiaceae (including genera *Cyanobium PCC-6307*, *Synechococcus CC9902*, *Planktothrix NIVA-CYA 15*) have been reported to prefer to develop on the surface of saltmarsh tidal mudflats [7, 48]. Taken together, these results suggest that tidal fluctuations have posed a domain-level community-specific influence on the transport mechanisms of Archaea and Bacteria. This discrepancy may also be related to the fact that archaeal communities prefer to live in the subsurface sediment, while bacteria have a wider niche breadth than archaea in the intertidal zone [49].

Especially, based on the hourly time-series sampling of intertidal surface water during whole tidal cycles, we have further found that periodic tidal fluctuations on a daily and monthly basis lead to the rhythm patterns of microbiota structure. The rhythmicity of environmental water microbiota has only been implicated in several long-term studies on the seasonal or circadian reoccurring patterns [50] of marine water

community structure or dynamics of individual prokaryotic taxa [39, 51]. Although the periodic shift in coastal microbiota structure associated with tidal fluctuation has been reported before through observation of a few discrete-time samples during tidal cycles [47], our results based on continuous time-series sampling demonstrated that tidal cycles dominated the rhythmic recurrent of not only groundwater-related microbiota during ebb tide but also seawater-related microbiota during flood tide. Further, by identifying the rhythmic species showing fluctuations in relative abundance in response to tidal cycles, we found that the rhythmic patterns observed in the whole prokaryotic communities were mainly dominated by the numerous and abundant rhythmic subcommunities. Intriguingly, the reoccurring period of rhythmic ASVs varied broadly from 10.69 to 49.86 hours, which may be due to the change of tidal periods in the investigated tidal creek resulting from tidal asymmetry (e.g., decrease in the duration of ebb and increase in the duration of flood) [52], as well as the hysteresis patterns on different time scales (e.g., diel and neap-spring) as suggested by prior hysteresis loops analysis of ^{222}Rn and greenhouse gas [35]. These first-hand results also enable our proposal of rhythmic ASVs with approximate periods of tidal cycles (~ 12 h) as potential microbial indicators of groundwater discharge (22 ASVs) and seawater intrusion (20 ASVs) in the coastal zone, respectively. Furthermore, the random forest models established based on the 42 rhythmic ASVs represented high predictive accuracy in physicochemical variables and great differentiation between ebb-tide and flood-tide surface water samples. Given that these variables, e.g., salinity, pH [53] and ^{222}Rn [54], were commonly used as environmental tracers to establish intertidal SGD or seawater intrusion in the coastal zone, our results demonstrated the potential of rhythmic prokaryotic species as new indicators of water quality (e.g., risk of seawater intrusion) in coastal ecosystems. Based on our discovery of microbiota rhythm patterns

in the examined coastal ecosystem and the nomination of generic microbial indicators, we propose to leverage the informatics of microbiota to add biologically relevant information to the monitoring and assessment of coastal ecosystem.

4.2. Homogeneous selection and biotic interactions co-contribute to the microbiota assembly in the natural intertidal water continuum

Given the tide-driven hydrodynamic disturbance and the accompanying environmental gradients across the temporal and spatial scales in the coastal zone [55], the corresponding ecological processes, i.e., selection and dispersal, are expected to play a key role in the microbiota assembly in the natural tidal creek. Despite microbial dispersal is expected to be enhanced under periodic tidal fluctuations, high levels of dispersal can result in a homogenization of the local and regional species pool, which can lead to an overall short-time increase in stochasticity (during initial formation phases of tidal creeks) followed by an increase in deterministic selection at a regional scale that decreases species diversity [56] (Fig. 1B). The resulting predominant contribution of homogeneous selection and relatively decreased dispersal limitation (representing intermediate dispersal rates) can lead to increased species competition, and augment the importance of drift (i.e., random birth and death events leading to rare species extinction). These results collectively account for the dominant contribution of homogeneous selection, drift and dispersal limitation in shaping microbiota structure (Fig. 4A) in the natural intertidal GW-SW continuum based on null model analyses, as well as species segregated distributions suggested by the C-score analyses.

While homogeneous selection predominated in groundwater and surface water, dispersal limitation (indicating higher dispersal rates) was weaker in the spring-tide surface water with stronger tidal fluctuations than the neap tide. Moreover, the increased homogeneous selection also agrees with stronger species segregation patterns

(negative biotic interactions) in surface water (Table S11) and the highest frequencies of species co-occurrence associations (mainly positive biotic interactions) in the spring-tide surface water (Fig. 6B). Compared with the surface water, weakening of water mixing disturbance in intertidal groundwater resulted from the barrier effect of cohesive sediment can account for the relatively lower dispersal rates. Meanwhile, among the tested physicochemical factors, salinity, pH, DO and dissolved carbon (DIC and DOC) mainly imposed homogeneous selection in shaping microbiota structure. We conclude that homogeneous selection (driven by abiotic factors) and biotic interactions co-contributed to the microbiota assembly patterns in the natural intertidal groundwater-surface water continuum.

4.3. Anthropogenic influences alter microbiota structure and community assembly patterns in intertidal groundwater

Intertidal zone harbors abundant and diverse microbial environments owing to the land-sea interaction and are extremely sensitive to natural changes and nearshore human activities [48, 57]. Nutrient loading derived from human activities or natural environments and tidal dynamics is among the critical pressures affecting the intertidal environments [58]. Based on the comparative microbiota analysis between the natural tidal creek (TC2) and a geographically adjacent (within 6 km) but human-influenced tidal creek (TC1), our study found that the human-influenced tidal creek exhibited both higher species diversity and community structural dissimilarities of groundwater microbiota than the natural one, whether for archaeal or bacterial communities. This contrasting profile is expected to result from the shift in groundwater microbiota structure caused by both terrestrial river-water input upstream (during ebb) and estuary-water input downstream (during flood tide) of the creek, suggesting an anthropogenic influence on intertidal groundwater microbiota.

Based on the null model, C-score and co-occurrence analyses of microbiota assembly mechanisms, we found that compared with the natural groundwater (TC2), the human-influenced groundwater (TC1) showed remarkably increased (and dominant) dispersal limitation, decreased homogeneous selection and drift, as well as stronger microbial co-occurrence patterns. First, the terrestrial river water input carries abundant nutrients from aquaculture and human activities, which can create additional niches to stimulate the growth of various microorganisms, especially less abundant ones. Such growth could increase species diversity (Fig. 1B) and enhance stochastic processes like birth and death, the latter of which is consistent with the increased co-contribution of dispersal limitation (the influence of dispersal limitation acting in concert with drift [23]) and drift (the influence of drift acting alone) in the human-influenced groundwater, as noticed in prior studies on terrestrial freshwater [59] and groundwater [13]. Second, nutrient inputs could weaken niche selection by providing more resources and result in less-stressed groundwater conditions, partly resulting in decreased homogeneous selection, which was mainly driven by nutrient-associated factors in the human-influenced groundwater, as suggested by the relationships between homogeneous selection and DIC or DOC (Fig. 5). Higher abundance of nitrogen-metabolizing genera, e.g., nitrifying *Nitrosopumilus* [60] and denitrifying *Hydrogenophag*a [61, 62], and carbon-metabolizing genera, e.g., *Bathyarchaeia* [63], and *Sphaerochaeta* [64] in the human-influenced than the natural groundwater (Fig. S13) further supported the important effect of nutrient input. Third, exogenous water inputs at ebb tide provided supplement water and therefore weakened tidal fluctuations (i.e., weakened groundwater discharge by rising surface water level), leading to the observed enhanced dispersal limitation. Further, our finding on the important role of stochastic processes (dispersal limitation in concert with drift) in controlling community assembly and

succession of the human-influenced groundwater microbiota is consistent with the prior experimental report indicating that stochasticity decreased, whereas niche selection could be stronger in a fluidic ecosystem with a disturbance, in turn, stochasticity increases after adding exogenous nutrients [13].

Despite its lower relative importance of homogeneous selection (representing environmental filtering), the human-influenced groundwater microbiota showed both a higher degree of species segregation and higher frequencies of species co-occurrence associations, indicating stronger biotic interactions. On the one hand, higher dispersal limitation and potential higher strength of competition due to increased species diversity (more species with similar ecological niches) enhanced the species segregation distribution. On the other hand, complex physicochemical gradients (e.g., abundant nutrients, salinity and DOC) [65] created multiple niches that harbor various microbial groups with different metabolic capacities (Fig. S10) and in turn created opportunities for synergistic or other cooperative interactions (mutualistic and commensal metabolism cooperation), which was supported by enrichment of copiotrophic genera *Woesearchaeales* [66] (well known as 'ultramicroarchaea') and *Flavobacterium* [67] and more in the human-influenced groundwater (Fig. S13). Meanwhile, more keystone 'connectors' enhanced the stability of the community under higher level of microbial cooperation (reduce stability) [68] in the human-influenced groundwater. Overall, the enhanced biotic interaction is one of the essential ecological processes that cannot be ignored when exploring the microbiota assembly patterns in the human-influenced intertidal groundwater.

5. Conclusion

By overcoming obstacles of time-series sampling in the salt marsh, this study unravels the high-resolution rhythm patterns of microbiota structure in response to periodic tidal

fluctuations in the intertidal groundwater-surface water continuum where microbiota assembly was found to be dominantly driven by homogeneous selection. Nutrient loading and weakened hydrodynamic disturbance resulting from anthropogenic influence are demonstrated for the first time to remarkably alter the microbiota biodiversity, structure and assembly patterns in the intertidal groundwater. Our first use and innovative construction of random forest models based on only a few newly-discovered rhythmic species suggested that it is technically realistic to enhance coastal monitoring initiatives by incorporating microbiome observations (e.g., only a few key species) and future surveillance for ecological assessment, such as the risk of seawater intrusion. The results also reveal how human activities shift coastal groundwater microbiota, which in turn may affect the function and health of the coastal ecosystem, such as the microbially-driven biogeochemical cycling processes in the coastal zone. Altogether, this study can provide valuable insights into the bio-monitoring and conservation of coastal zone ecosystems.

Data Availability

The raw sequencing data generated in this study have been deposited in the China National GeneBank DataBase (CNGBdb) with accession number CNP0003642.

Acknowledgement

This work was supported by the Zhejiang Provincial Natural Science Foundation of China under Grant No. LR22D010001. We acknowledge the Research Center for Industries of the Future (RCIF) at Westlake University for support, and thank the Westlake University HPC Center for computational support. Thank Mr. Duofei Hu and Ms. Shengjie Hu for assistance in field sampling, and Ms. Yisong Xu for laboratory management supports.

Author Contributions

All authors contributed intellectual input and assistance to this study. The original concepts were conceived by F.J. and Z.Z. with advice from L.L. Field sampling was carried out by Z.Z. and X.C. Data analysis were done by Z.Z. with assistance from G.Z. The manuscript was prepared by Z.Z. and F.J. and revised by L.L., L.Z. and H.G. F.J. supervised the project.

Competing Interests

The authors declare no competing interests.

References

1. Heckbert S, Costanza R, Poloczanska ES, Richardson AJ. Climate Regulation as a Service from Estuarine and Coastal Ecosystems. In: Wolanski E, McLusky D, editors. Treatise on Estuarine and Coastal Science. Waltham: Academic Press; 2011. p. 199-216.
2. Xin P, Wilson A, Shen CJ, Ge ZM, Moffett KB, Santos IR, et al. Surface Water and Groundwater Interactions in Salt Marshes and Their Impact on Plant Ecology and Coastal Biogeochemistry. Rev Geophys. 2022;60(1).
3. Santoro AE. Microbial nitrogen cycling at the saltwater-freshwater interface. Hydrogeol J. 2010;18(1):187-202.
4. Mayfield KK, Eisenhauer A, Santiago Ramos DP, Higgins JA, Horner TJ, Auro M, et al. Groundwater discharge impacts marine isotope budgets of Li, Mg, Ca, Sr, and Ba. Nat Commun. 2021;12(1):148.
5. Hwang DW, Lee YW, Kim G. Large submarine groundwater discharge and benthic eutrophication in Bangdu Bay on volcanic Jeju Island, Korea. Limnol Oceanogr. 2005;50(5):1393-403.
6. Ruiz-Gonzalez C, Rodellas V, Garcia-Orellana J. The microbial dimension of submarine groundwater discharge: current challenges and future directions. FEMS Microbiol Rev. 2021;45(5).
7. Hong Y, Wu J, Wilson S, Song B. Vertical Stratification of Sediment Microbial Communities Along Geochemical Gradients of a Subterranean Estuary Located at the Gloucester Beach of Virginia, United States. Front Microbiol. 2018;9:3343.
8. Adyasari D, Hassenruck C, Oehler T, Sabdaningsih A, Moosdorf N. Microbial community structure associated with submarine groundwater discharge in northern Java (Indonesia). Sci Total Environ. 2019;689:590-601.
9. Sang SL, Dai H, Hu BX, Hao YR, Zhou T, Zhang J. The Study of Hydrogeochemical Environments and Microbial Communities along a Groundwater Salinity Gradient in the Pearl River Delta, China.

Water-Sui. 2019;11(4).
10. Chen L, Zhang J, Dai H, Hu BX, Tong J, Gui D, et al. Comparison of the groundwater microbial community in a salt-freshwater mixing zone during the dry and wet seasons. J Environ Manage. 2020;271:110969.
11. Chen X, Ye Q, Sanders CJ, Du J, Zhang J. Bacterial-derived nutrient and carbon source-sink behaviors in a sandy beach subterranean estuary. Mar Pollut Bull. 2020;160:111570.
12. Chen YJ, Leung PM, Cook PLM, Wong WW, Hutchinson T, Eate V, et al. Hydrodynamic disturbance controls microbial community assembly and biogeochemical processes in coastal sediments. Isme J. 2022;16(3):750-63.
13. Zhou J, Deng Y, Zhang P, Xue K, Liang Y, Van Nostrand JD, et al. Stochasticity, succession, and environmental perturbations in a fluidic ecosystem. Proc Natl Acad Sci U S A. 2014;111(9):E836-45.
14. Hanley TC, Bowen JL, Kearns PJ, Hughes AR. Short- and long-term effects of nutrient enrichment on salt marsh plant production and microbial community structure. Journal of Ecology. 2021;109(11):3779-93.
15. Yao Z, Du S, Liang C, Zhao Y, Dini-Andreote F, Wang K, et al. Bacterial Community Assembly in a Typical Estuarine Marsh with Multiple Environmental Gradients. Appl Environ Microbiol. 2019;85(6).
16. Adyasari D, Hassenruck C, Montiel D, Dimova N. Microbial community composition across a coastal hydrological system affected by submarine groundwater discharge (SGD). Plos One. 2020;15(6):e0235235.
17. Zhang G, Bai J, Tebbe CC, Zhao Q, Jia J, Wang W, et al. Salinity controls soil microbial community structure and function in coastal estuarine wetlands. Environ Microbiol. 2021;23(2):1020-37.
18. Chave J. Neutral theory and community ecology. Ecology Letters. 2004;7(3):241-53.
19. Vellend M. Conceptual synthesis in community ecology. Q Rev Biol. 2010;85(2):183-206.
20. Nemergut DR, Schmidt SK, Fukami T, O'Neill SP, Bilinski TM, Stanish LF, et al. Patterns and processes of microbial community assembly. Microbiol Mol Biol Rev. 2013;77(3):342-56.
21. Zhou J, Ning D. Stochastic Community Assembly: Does It Matter in Microbial Ecology? Microbiol Mol Biol Rev. 2017;81(4).
22. Ning D, Yuan M, Wu L, Zhang Y, Guo X, Zhou X, et al. A quantitative framework reveals ecological drivers of grassland microbial community assembly in response to warming. Nat Commun. 2020;11(1):4717.
23. Stegen JC, Lin X, Fredrickson JK, Chen X, Kennedy DW, Murray CJ, et al. Quantifying community assembly processes and identifying features that impose them. Isme J. 2013;7(11):2069-79.
24. Gao GF, Peng D, Zhang Y, Li Y, Fan K, Tripathi BM, et al. Dramatic change of bacterial assembly process and co-occurrence pattern in Spartina alterniflora salt marsh along an inundation frequency gradient. Sci Total Environ. 2021;755(Pt 1):142546.
25. Gao GF, Peng D, Tripathi BM, Zhang Y, Chu H. Distinct Community Assembly Processes of Abundant and Rare Soil Bacteria in Coastal Wetlands along an Inundation Gradient. mSystems. 2020;5(6).
26. Wang K, Yan H, Peng X, Hu H, Zhang H, Hou D, et al. Community assembly of bacteria and archaea in coastal waters governed by contrasting mechanisms: A seasonal perspective. Mol Ecol.

2020;29(19):3762-76.
27. Kraft NJB, Adler PB, Godoy O, James EC, Fuller S, Levine JM. Community assembly, coexistence and the environmental filtering metaphor. Funct Ecol. 2015;29(5):592-9.
28. Faust K, Raes J. Microbial interactions: from networks to models. Nat Rev Microbiol. 2012;10(8):538-50.
29. Berry D, Widder S. Deciphering microbial interactions and detecting keystone species with co-occurrence networks. Front Microbiol. 2014;5:219.
30. Yuan MM, Guo X, Wu LW, Zhang Y, Xiao NJ, Ning DL, et al. Climate warming enhances microbial network complexity and stability. Nature Climate Change. 2021;11(4):343-U100.
31. Ju F, Xia Y, Guo F, Wang Z, Zhang T. Taxonomic relatedness shapes bacterial assembly in activated sludge of globally distributed wastewater treatment plants. Environ Microbiol. 2014;16(8):2421-32.
32. Ju F, Zhang T. Bacterial assembly and temporal dynamics in activated sludge of a full-scale municipal wastewater treatment plant. Isme J. 2015;9(3):683-95.
33. Niederdorfer R, Fragner L, Yuan L, Hausherr D, Wei J, Magyar P, et al. Distinct growth stages controlled by the interplay of deterministic and stochastic processes in functional anammox biofilms. Water Res. 2021;200:117225.
34. Shen Y, Feng N-h, Zhou Q, Liu Y-m, Chen Z-y. The status and its influence of reclamation on Jiangsu coast. Marine Sciences. 2006;10:008.
35. Chen XG, Santos IR, Hu DF, Zhan LC, Zhang Y, Zhao Z, et al. Pore-water exchange flushes blue carbon from intertidal saltmarsh sediments into the sea. Limnol Oceanogr Lett. 2022;7(4):312-20.
36. Bolyen E, Rideout JR. Reproducible, interactive, scalable and extensible microbiome data science using QIIME 2. Nature Biotechnology. 2019;37(8):852-7.
37. McMurdie PJ, Holmes S. phyloseq: an R package for reproducible interactive analysis and graphics of microbiome census data. Plos One. 2013;8(4):e61217.
38. Liu C, Cui Y, Li X, Yao M. microeco: an R package for data mining in microbial community ecology. FEMS Microbiol Ecol. 2021;97(2):fiaa255.
39. Lambert S, Tragin M, Lozano JC, Ghiglione JF, Vaulot D, Bouget FY, et al. Rhythmicity of coastal marine picoeukaryotes, bacteria and archaea despite irregular environmental perturbations. Isme J. 2019;13(2):388-401.
40. Letunic I, Bork P. Interactive Tree Of Life (iTOL) v5: an online tool for phylogenetic tree display and annotation. Nucleic Acids Res. 2021;49(W1):W293-W6.
41. Kolde R, Kolde MR. Package 'pheatmap'. R package. 2015;1(7):790.
42. Stone L, Roberts A. The checkerboard score and species distributions. Oecologia. 1990;85(1):74-9.
43. Hu A, Ju F, Hou L, Li J, Yang X, Wang H, et al. Strong impact of anthropogenic contamination on the co-occurrence patterns of a riverine microbial community. Environ Microbiol. 2017;19(12):4993-5009.
44. Deng Y, Jiang YH, Yang Y, He Z, Luo F, Zhou J. Molecular ecological network analyses. BMC Bioinformatics. 2012;13:113.
45. Zhou J, Deng Y, Luo F, He Z, Tu Q, Zhi X. Functional molecular ecological networks. Mbio. 2010;1(4).

46. Eglen RM, Whiting RL. Competitive and non-competitive antagonism exhibited by 'selective' antagonists at atrial and ileal muscarinic receptor subtypes. British Journal of Pharmacology. 1987;90(4):701-7.
47. Lee E, Shin D, Hyun SP, Ko KS, Moon HS, Koh DC, et al. Periodic change in coastal microbial community structure associated with submarine groundwater discharge and tidal fluctuation. Limnol Oceanogr. 2017;62(2):437-51.
48. Stal LJ. Microphytobenthos as a biogeomorphological force in intertidal sediment stabilization. Ecol Eng. 2010;36(2):236-45.
49. Chen W, Wen D. Archaeal and bacterial communities assembly and co-occurrence networks in subtropical mangrove sediments under Spartina alterniflora invasion. Environ Microbiome. 2021;16(1):10.
50. Fuhrman JA, Cram JA, Needham DM. Marine microbial community dynamics and their ecological interpretation. Nat Rev Microbiol. 2015;13(3):133-46.
51. Auladell A, Barberan A, Logares R, Garces E, Gasol JM, Ferrera I. Seasonal niche differentiation among closely related marine bacteria. Isme J. 2022;16(1):178-89.
52. Blanton JO, Lin GQ, Elston SA. Tidal current asymmetry in shallow estuaries and tidal creeks. Cont Shelf Res. 2002;22(11-13):1731-43.
53. Werner AD, Bakker M, Post VEA, Vandenbohede A, Lu CH, Ataie-Ashtiani B, et al. Seawater intrusion processes, investigation and management: Recent advances and future challenges. Advances in Water Resources. 2013;51:3-26.
54. Zhong Q, Wang X, Wang Q, Zhang F, Li L, Wang Y, et al. (222)Rn, (210)Pb and (210)Po in coastal zone groundwater: Activities, geochemical behaviors, consideration of seawater intrusion effect, and the potential radiation human-health risk. Appl Radiat Isot. 2020;166:109386.
55. Martiny JB, Eisen JA, Penn K, Allison SD, Horner-Devine MC. Drivers of bacterial beta-diversity depend on spatial scale. Proc Natl Acad Sci U S A. 2011;108(19):7850-4.
56. Custer GF, Bresciani L, Dini-Andreote F. Ecological and Evolutionary Implications of Microbial Dispersal. Front Microbiol. 2022;13:855859.
57. McCall BD, Pennings SC. Geographic variation in salt marsh structure and function. Oecologia. 2012;170(3):777-87.
58. Li H, Chi Z, Li J, Wu H, Yan B. Bacterial community structure and function in soils from tidal freshwater wetlands in a Chinese delta: Potential impacts of salinity and nutrient. Sci Total Environ. 2019;696:134029.
59. Ren LJ, He D, Chen Z, Jeppesen E, Lauridsen TL, Sondergaard M, et al. Warming and nutrient enrichment in combination increase stochasticity and beta diversity of bacterioplankton assemblages across freshwater mesocosms. Isme J. 2017;11(3):613-25.
60. Walker CB, de la Torre JR, Klotz MG, Urakawa H, Pinel N, Arp DJ, et al. Nitrosopumilus maritimus genome reveals unique mechanisms for nitrification and autotrophy in globally distributed marine crenarchaea. Proc Natl Acad Sci U S A. 2010;107(19):8818-23.
61. Willems A, Gillis M. Hydrogenophaga. Bergey's Manual of Systematics of Archaea and Bacteria. 2015:1-15.

62. Willems A, Busse J, Goor M, Pot B, Falsen E, Jantzen E, et al. Hydrogenophaga, a New Genus of Hydrogen-Oxidizing Bacteria That Includes Hydrogenophaga flava comb. nov. (Formerly Pseudomonas flava), Hydrogenophaga palleronii (Formerly Pseudomonas palleronii), Hydrogenophaga pseudoflava (Formerly Pseudomonas pseudoflava and "Pseudomonas carboxy do flava"), and Hydrogenophaga taeniospiralis (Formerly Pseudomonas taeniospiralis). Int J Syst Evol Micr. 1989;39(3):319-33.
63. Romano RG, Bendia AG, Moreira JCF, Franco DC, Signori CN, Yu TT, et al. Bathyarchaeia occurrence in rich methane sediments from a Brazilian ria. Estuar Coast Shelf S. 2021;263.
64. Oshurkova V, Troshina O, Trubitsyn V, Ryzhmanova Y, Bochkareva O, Shcherbakova V. Characterization of Methanosarcina mazei JL01 Isolated from Holocene Arctic Permafrost and Study of the Archaeon Cooperation with Bacterium Sphaerochaeta associata GLS2T. Proceedings. 2020;66(1):4.
65. Veach AM, Stegen JC, Brown SP, Dodds WK, Jumpponen A. Spatial and successional dynamics of microbial biofilm communities in a grassland stream ecosystem. Mol Ecol. 2016;25(18):4674-88.
66. Liu X, Li M, Castelle CJ, Probst AJ, Zhou Z, Pan J, et al. Insights into the ecology, evolution, and metabolism of the widespread Woesearchaeotal lineages. Microbiome. 2018;6(1):102.
67. Ho A, Di Lonardo DP, Bodelier PLE. Revisiting life strategy concepts in environmental microbial ecology. FEMS Microbiology Ecology. 2017;93(3).
68. Ya T, Du S, Li ZY, Liu SD, Zhu MH, Liu XJ, et al. Successional Dynamics of Molecular Ecological Network of Anammox Microbial Communities under Elevated Salinity. Water Research. 2021;188.

Figure and Table Legends

Fig. 1. Sampling and overview of archaeal and bacterial communities in tidal creek groundwater and surface water. (A) Map of two salt marsh tidal creeks (TC1 and TC2) sampled in this study. (B) Alpha diversity shown as ACE and Shannon indices. (C) The composition of phylum-level archaeal and bacterial communities.

Fig. 2. The structural variations of microbial communities within and between tidal creek groundwater and surface water. The non-multidimensional scaling (NMDS) ordination based on weighted UniFrac distance is employed to characterize the compositional variations of archaeal (A) and bacterial (B) communities in TC1-PW, TC2-PW, TS-Ebb/Flood (left figures) or TS-Neap/Spring (right figures).

Fig. 3. Rhythmicity of microbiota in tidal creek surface water. (A) The NMDS ordination of prokaryotic (archaeal and bacterial) communities in tidal creek surface water is displayed and trajectories show sampling order of surface water during neap tide and spring tide. (B) Pairwise comparisons of environmental factors are shown with a color gradient denoting Spearman's correlation. Microbiota composition in TS-Neap, TS-Spring and TS groups was related to each factor by partial mantel tests. (C) NMDS ordination of rhythmic subcommunities and non-rhythmic subcommunities in creek surface water. (D) Temporal abundance trends of representative ASVs (top5 with higher relative abundance) with a rhythmic period between 10 to 14 hours.

Fig. 4. Community assembly processes across different phylogenetic groups. (A) Relative importance of five ecological processes across groups, including heterogeneous selection (HeS), homogeneous selection (HoS), dispersal limitation (DL), homogenizing dispersal (HD), and drift and others (DR). (B) Phylogenetic tree of top member lineage in each Bin was displayed at class-level. Relative abundance of each Bin was displayed in first rectangle. Dominant processes in each Bin (colored

rectangle) and Bin contribution (stacked bars) to major ecological processes (HoS, DL and DR) in TC2-PW, TS-Neap and TS-Spring were displayed in 2-5 annulus. **C** Bin-class (top15 and others) contributions to the major ecological processes.

Fig. 5. Effects of environmental factors on major ecological processes. Heatmap plot of correlations between environmental factors and dominant ecological processes based on mantel test. The correlation was determined based on the difference (with a 'd' before the factors) or the mean (with a 'm' before the factors) of a factor between each pair of samples.

Fig. 6. Microbial segregation and co-occurrence patterns of tidal creek water microbiota. (A) Standardized effect sizes (SES) values of C-score and Cvar-score for intertidal groundwater and surface water microbiota over six groups. (B) Microbial co-occurrence networks in groundwater and surface water groups.

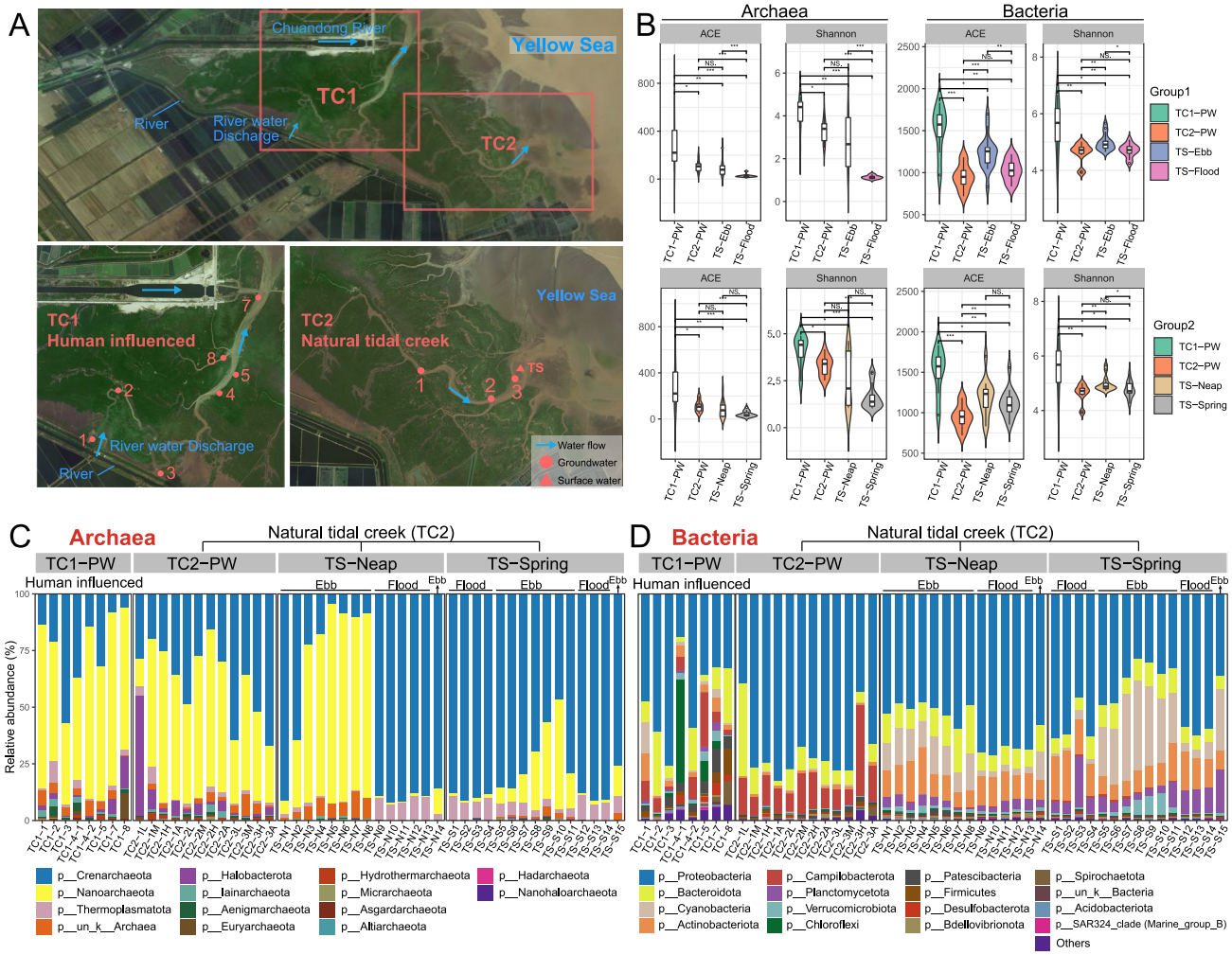

Figure 1. Sampling and overview of archaeal and bacterial communities in tidal creek groundwater and surface water. (A) Map of two salt marsh tidal creeks (TC1 and TC2) sampled in this study. Red rectangle in the figure above marks the two tidal creeks. Red dots in the bottom figure show the sampling sites of intertidal groundwater within TC1 and TC2. Red triangle within TC2 shows the sampling site of times series station. Blue arrows show the water flow direction of terrestrial Chuandong river and tidal creek, as well as the terrestrial river water input upstream of TC1. (B) Alpha diversity shown as ACE and Shannon indices. The significance level in the median differences across groups is statistically checked using wilcoxon rank-sum tests. Significance is expressed as ***$p < 0.001$, **$p < 0.01$, *$p < 0.05$, NS-non significant. (C) The composition of phylum-level archaeal and bacterial communities.

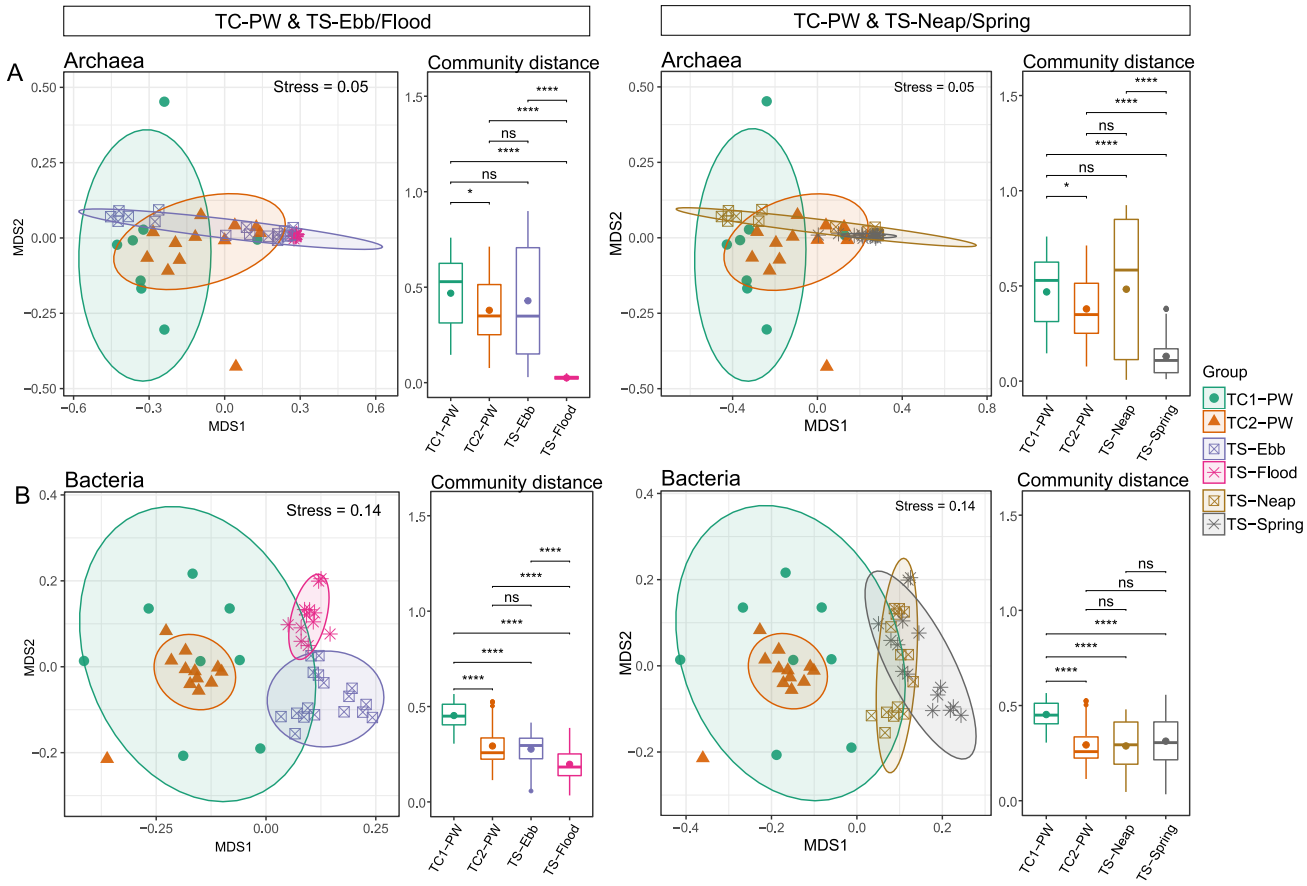

Figure 2. The structural variations of microbial communities within and between tidal creek groundwater and surface water. The non-multidimensional scaling (NMDS) ordination based on weighted UniFrac distance is employed to characterize the compositional variations of archaeal (A) and bacterial (B) communities in TC1-PW, TC2-PW, TS-Ebb/Flood (left figures) or TS-Neap/Spring (right figures). The archaeal and bacterial community distance across groups based on weighted UniFrac distance is displayed (right panel) and statistically significant differences across groups are calculated based on wilcoxon rank-sum test (****$p < 0.0001$, ***$p < 0.001$, **$p < 0.01$, *$p < 0.05$, ns-non significant).

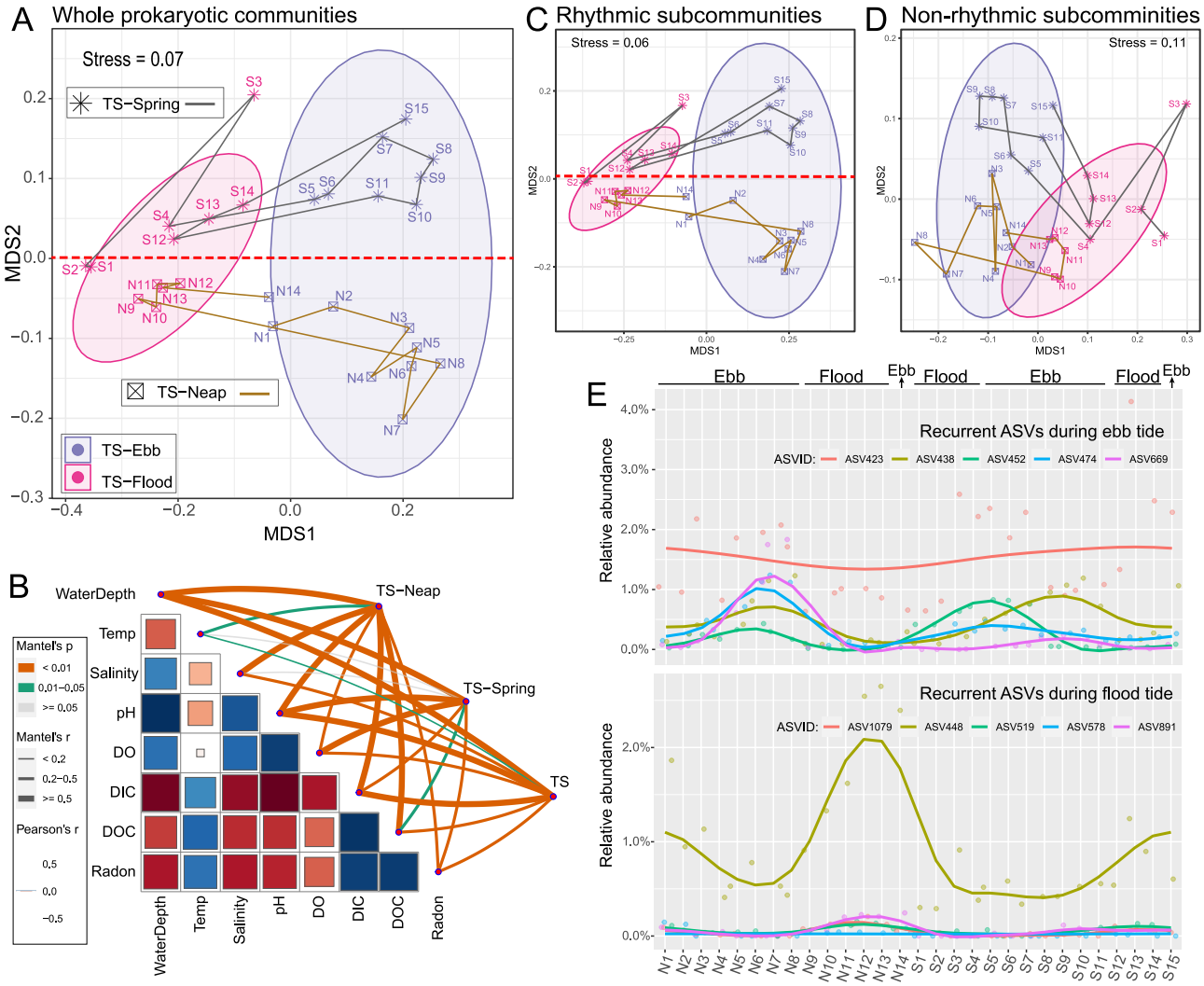

Figure 3. Rhythmicity of microbiota in tidal creek surface water. (A) The NMDS ordination of prokaryotic (archaeal and bacterial) communities in tidal creek surface water is displayed and trajectories show sampling order of surface water during neap tide (N1-N14 with brown lines) and spring tide (S1-S15 with gray lines). The pink and purple ellipses mark surface water samples collecting during flood tide and ebb tide, respectively. (B) Pairwise comparisons of environmental factors are shown with a color gradient denoting Spearman's correlation. Microbiota composition in TS-Neap, TS-Spring and TS groups was related to each factor by partial mantel tests. Edge width corresponds to the mantel's r statistic for the corresponding distance correlations and edge color denotes the statistical significance based on 9,999 permutations. (C) NMDS ordination of rhythmic subcommunities and non-rhythmic subcommunities in creek surface water. (D) Temporal abundance trends of representative ASVs (top5 with higher relative abundance) with a rhythmic period between 10 to 14 hours and these ASVs were classified according to the detection of higher recurrent signal at ebb tide or flood tide. A generalized additive model smooth is adjusted to the data points.

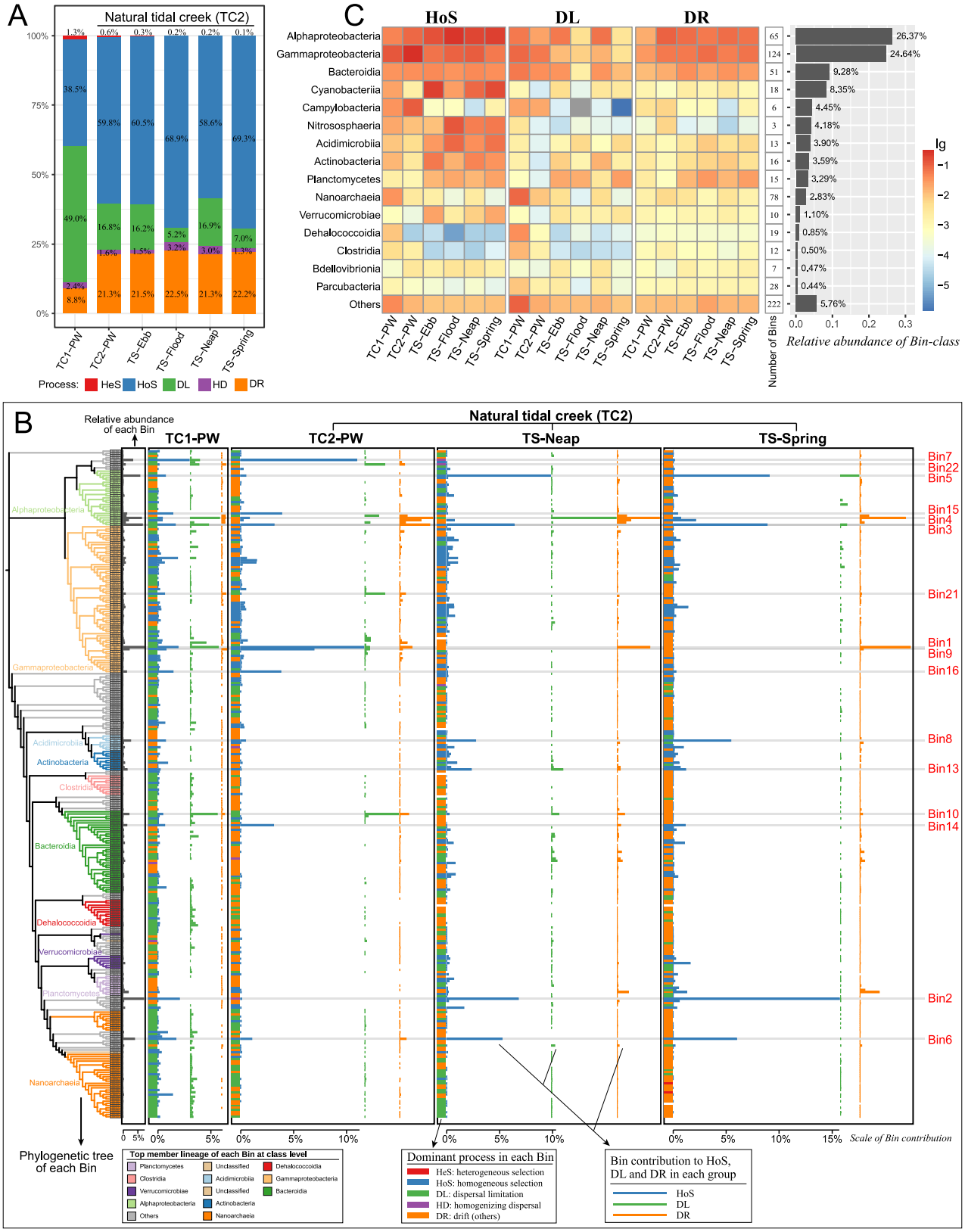

Figure 4. Community assembly processes across different phylogenetic groups. (A) Relative importance of five ecological processes across groups, including heterogeneous selection (HeS), homogeneous selection (HoS), dispersal limitation (DL), homogenizing dispersal (HD), and drift and others (DR). (B) Phylogenetic tree of top member lineage in each Bin was displayed at class-level. Relative abundance of each Bin was displayed in first rectangle. Dominant processes in each Bin (colored rectangle) and Bin contribution (stacked bars) to major ecological

processes (HoS, DL and DR) in TC2-PW, TS-Neap and TS-Spring were displayed in 2-5 annulus. Top Bins with higher contribution to ecological processes were marked by gray strip. Only the top300 Bins were shown in this figure, accounting for a relative abundance of 96.1% of all Bins. (C) Bin-class (top15 and others) contributions to the major ecological processes (HoS, DL, and DR) were displayed in the left heatmap. Sum of relative abundance of all Bins in each Bin-class was displayed in right bar chart. The vertical numbers at the right of the heatmap showed the number of Bins classified at class-level.

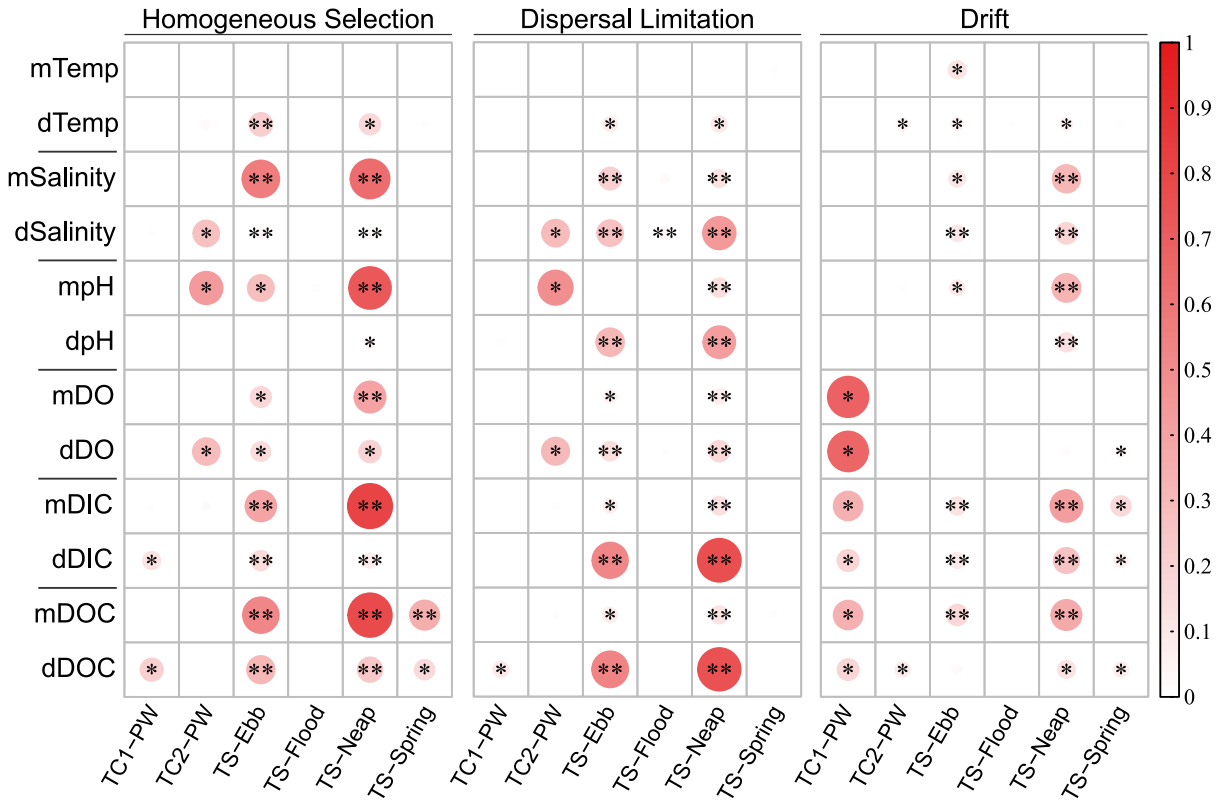

Figure 5. Effects of environmental factors on major ecological processes. Heatmap plot of correlations between environmental factors and dominant ecological processes based on mantel test. The correlation was determined based on the difference (with a 'd' before the factors) or the mean (with a 'm' before the factors) of a factor between each pair of samples. Significance was expressed as $^{**}P < 0.01$, $^{*}P < 0.05$.

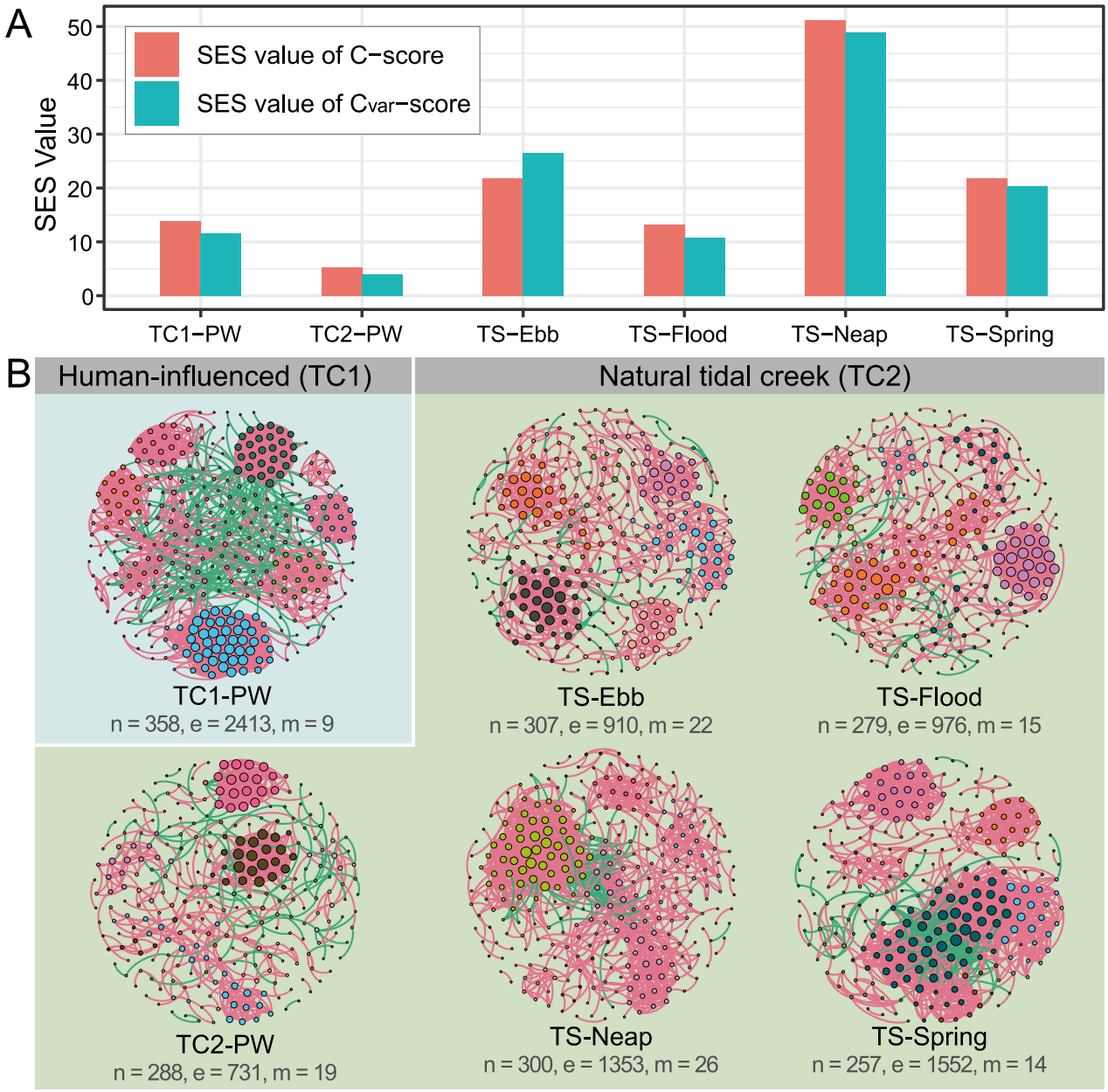

Figure 6. Microbial segregation and co-occurrence patterns of tidal creek water microbiota. (A) Standardized effect sizes (SES) values of C-score and C_{var}-score for intertidal groundwater and surface water microbiota over six groups. Higher observed SES values of C-score suggest greater degrees of species segregation than would be expected by chance. Higher SES values of Cvar-score indicate greater degrees of both species segregation and aggregation. All *P*-values are < 0.0001 (detailed in Text S5 and Table S12). (B) Microbial co-occurrence networks in groundwater and surface water groups. n: number of nodes; e: number of edges; m: number of modules. The networks are colored by modularity. More details are described in Text S6 and Table S13.